Particle acceleration in winds of star clusters

Giovanni Morlino

INAF/Osservatorio astrofisico di Arcetri

Firenze (ITALY)

Paris Saclay AstroParticle Symposium, 18 Oct- 28 Nov 2021 - Paris

NGC 2237-9 The Rosette Nebula

Where does PeV particles come from?

In spite of big efforts of the last years, the origin of CRs is still unclear

- The SNR paradigm is the most accepted scenario but
  - problem in reaching the maximum energy close to ~PeV for protons [see Cristofari, Blasi, Amato 2020]
  - issue concerning the chemical abundances (e.g. $^{20}Ne/^{22}Ne$) [see Prantzos, 2012, A&A 538]

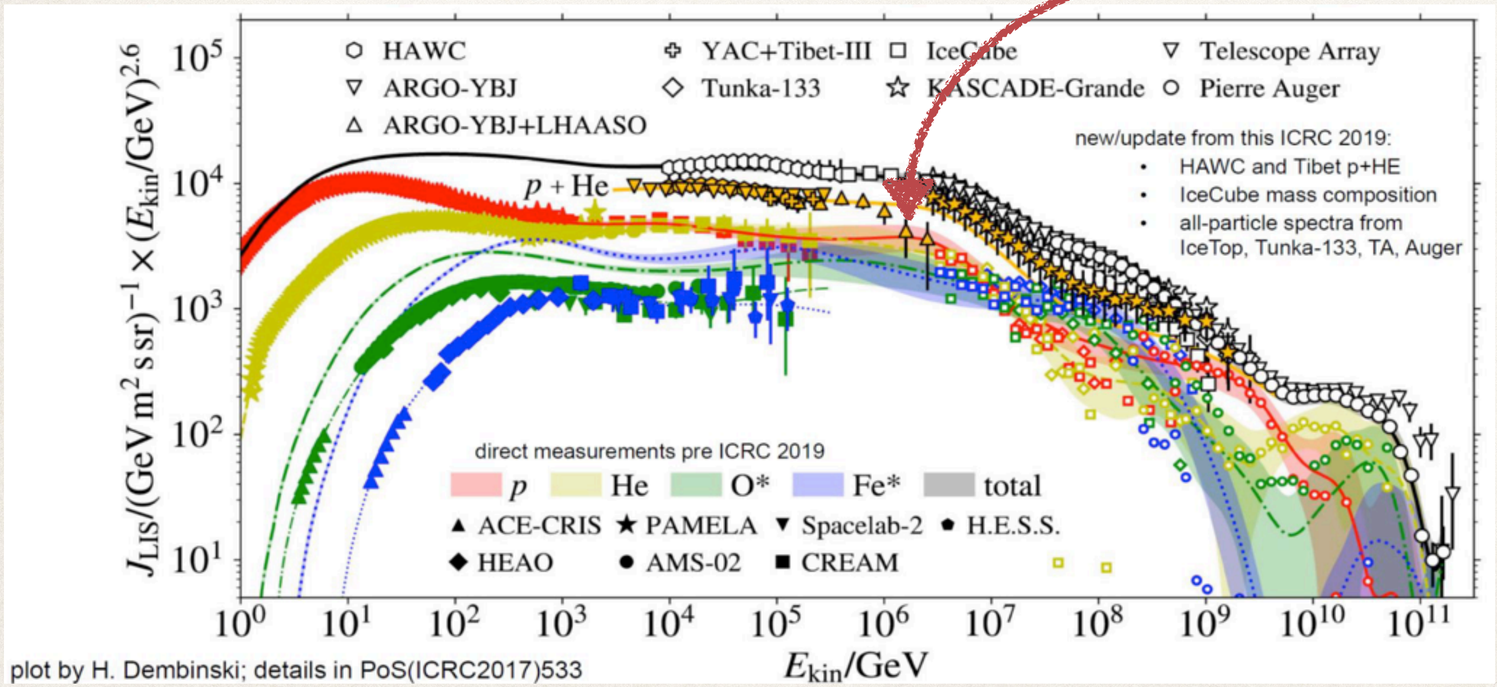

Galactic CR protons should be accelerated up to ~PeV to explain the knee in the CR spectrum

It is worth exploring other possible candidates for the production of cosmic rays

Stellar winds represent the second most powerful source

Luminosity of stellar winds

[Cesarsky & Montmerle, 1983; Seo, Kang & Ryu, 2018]

Power in stellar winds

$$P_{SW} = \int_{M_{\rm min}}^{M_{\rm max}} \xi(M)\, \mathscr{L}_w(M)\, \tau_s(M)\, dM$$

$$M_{\rm min} = 0.08 M_\odot;\ M_{\rm max} = 110 M_\odot$$

Initial mass function

$$\xi(M) = \frac{dN}{dM} \propto M^{-2.35}$$ [Salpeter, 1955]

Wind kinetic luminosity

$$\mathscr{L}_w = \frac{1}{2}\dot{M}\, v_w^2$$

Star main sequence lifetime

$$\tau_s(M) \simeq \tau_\odot \left(\frac{M}{M_\odot}\right)^{-2.5}$$

Mass loss rate

$$\dot{M} = 9.6 \times 10^{-15} \left(\frac{L}{L_\odot}\right)^{1.45} \left(\frac{M}{M_\odot}\right)^{0.16} \left(\frac{R}{R_\odot}\right)^{0.81}$$

[Nieuwenhuijzen & de Jager, 1990]

Stellar wind speed

$$v_w \gtrsim v_\infty = \sqrt{2GM/R_s}$$

Power in SN explosion

$$P_{SN} = E_{\rm SN} \int_{M_s}^{M_{\rm max}} \xi(M)\, dM$$

$$E_{\rm SN} = 10^{51}\ {\rm erg/s}$$

$$M_s \simeq 8\, M_\odot$$

Ratio:

$$\left(\frac{P_{SW}}{P_{SN}}\right) \approx 0.2 \ \in [0.06, 3]$$

Stellar wind power can be comparable with the SN Power
but there are numerous uncertainties

(I am neglecting the role of WR stars)

Luminosity of stellar winds

[Seo, Kang & Ryu, 2018]

Power in stellar winds for different stellar phases

$$\mathcal{L}_{w,MS_B} = 3.2 \times 10^{36}\,\mathrm{erg/s}$$

$$\mathcal{L}_{w,MS_O} = 7.3 \times 10^{40}\,\mathrm{erg/s}$$

$$\mathcal{L}_{w,\mathrm{RSG}} = 7.5 \times 10^{36}\,\mathrm{erg/s}$$

$$\mathcal{L}_{w,\mathrm{WR}} = 4.1 \times 10^{40}\,\mathrm{erg/s}$$

Wind luminosity of single stars

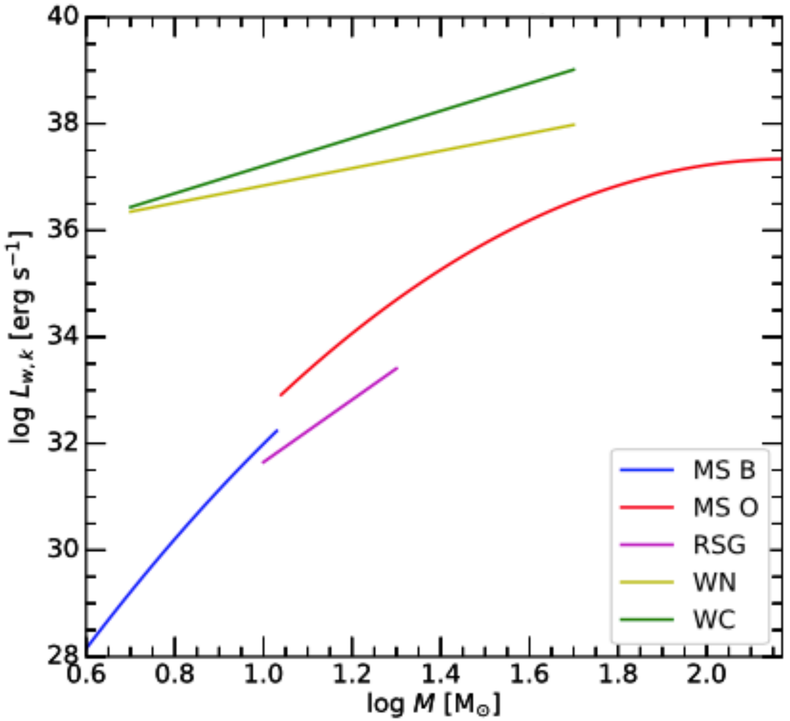

Wind luminosity integrated over Galactic population

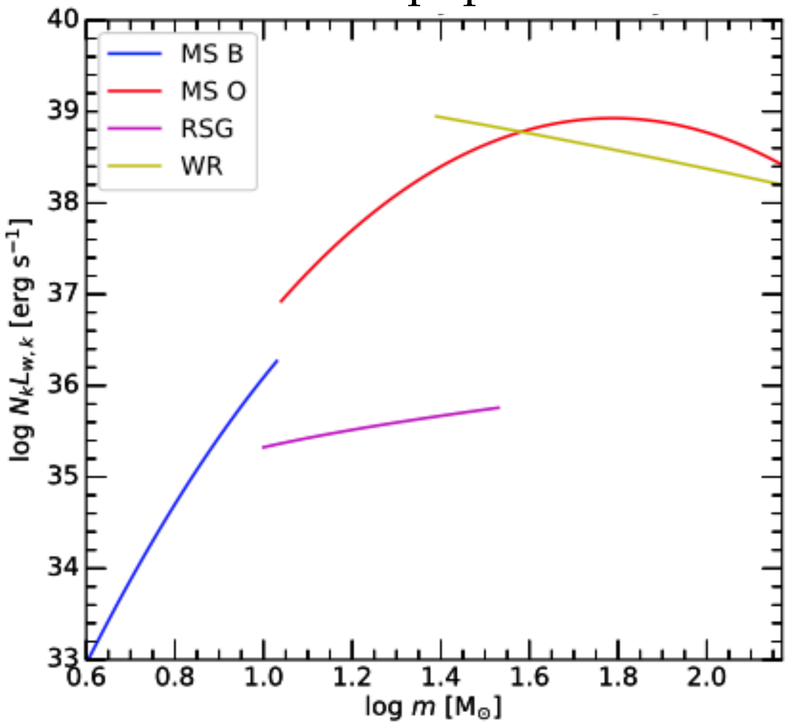

Main sequence O stars and Wolf-Rayet stars are the dominant sources

Hints from CR chemical composition

- **In the CR spectrum the $^{22}Ne/^{20}Ne$ ~ 5 times the Solar value**
- The only place where **^{22}Ne** is overabundant is the stellar external layers of massive stars
- In past this argument was used in favour of CR acceleration in super bubbles [Higdon & Lingenfelter 2003; Bings et al 2003, 2008] but in fact the average **$^{22}Ne/^{20}Ne$** in SB is roughly Solar (enriched by winds but also by SN ejecta) [Prantzos, 2012]
- Stellar rotation can mix the outer layers ⇒ **^{22}Ne** enrichment of stellar wind ⇒ preferential acceleration of stellar wind material can solve the problem
- **From abundances of CR species, Tatischeff et al. MNRAS 508, (2021) inferred that ~6% of (low energy) CR should come from SW material**
- Uncertainties due to several factors (e.g. element mixing in stellar layers, ionisation level, etc.)

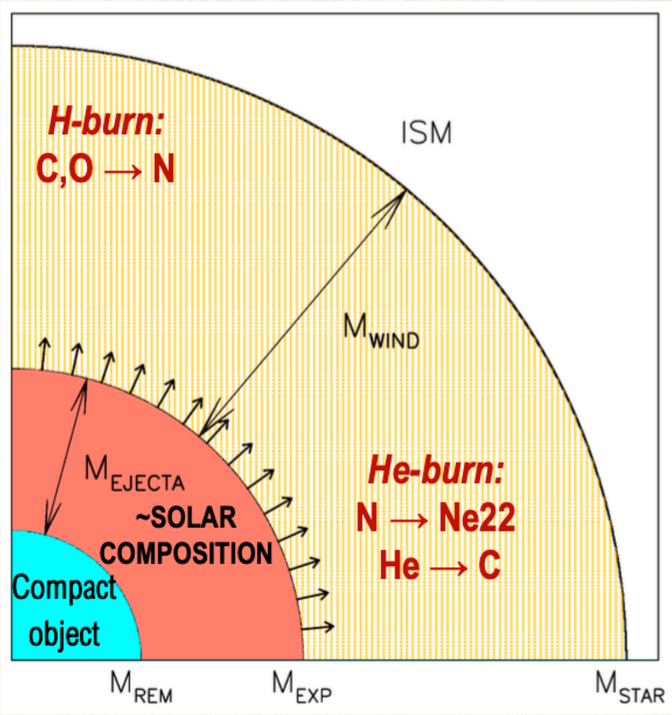

Different role of stellar winds

WINDS FROM SINGLE STARS

Pros.

- Winds from massive stars inject into the Galaxy a kinetic energy comparable to SNRs [Cesarsky & Montmerle, 1983]
- Long-living systems (age ~ Myr)
- Large size (bubble can reach several tens of pc)

Cons.

- Small velocity ($v_w \lesssim 3000$ km/s)
- Small mass ejecta: $\dot{M} \lesssim 10^{-6}\, M_\odot\, \mathrm{yr}^{-1}$
- Small magnetic field in the free wind region $\rightarrow$ large diffusion coefficient $\rightarrow$ small $E_{\max}$

WIND FROM MASSIVE YOUNG STELLAR CLUSTERS

- $\#\mathrm{stars} \gtrsim 10^3 \;\Rightarrow\; \dot{M} \gtrsim 10^{-4} M_\odot\, \mathrm{yr}^{-1}$
- presence of strong wind turbulence $\Rightarrow$ possibility to generate magnetic turbulence

Massive stellar clusters detected in gamma-rays

Recently, several young massive stellar clusters have been associated with gamma-rays sources

Name	log M/M_{sun}	r_c/pc	D/kpc	age/Myr	L_w/ 10^{38} erg s^{-1}	Reference
Westerlund 1	4.6 ± 0.045	1.5	4	4-6	10	Abramowski A., et al., 2012, A&A, 537, A114
Westerlund 2	4.56 ±0.035	1.1	2.8 ± 0.4	1.5-2.5	2	Yang, de Oña Wilhelmi, Aharonian, 2018, A&A, 611, A77
Cyg. OB2	4.7±0.3	5.2	1.4	3-6	2	Ackermann M., et al. 2011, Science, 334, 1103
NGC 3603	4.1 ± 0.10	1.1	6.9	2-3	?	Saha, L. et al 2020, ApJ, 897, 131
BDS 2003	4.39	0.2	4	1	?	Albert A., et al., 2020, arXiv:2012.15275
W40	2.5	0.44	0.44	1.5	?	Sun, X.-N. et al. 2020, A&A, 639, A80
30 Dor (LMC) NGC 2070/RCM 136	4.8-5.7 4.34-5	multiple sub-clusters	50	1 5	?	H. E. S. S. Collaboration et al., 2015, Science, 347, 406

OBSERVATIONS: Cygnus OB2

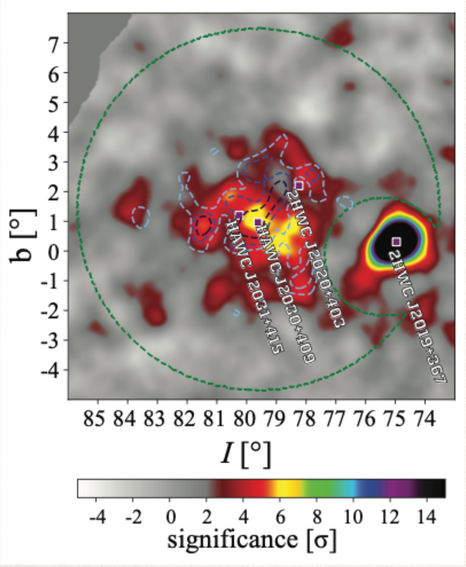

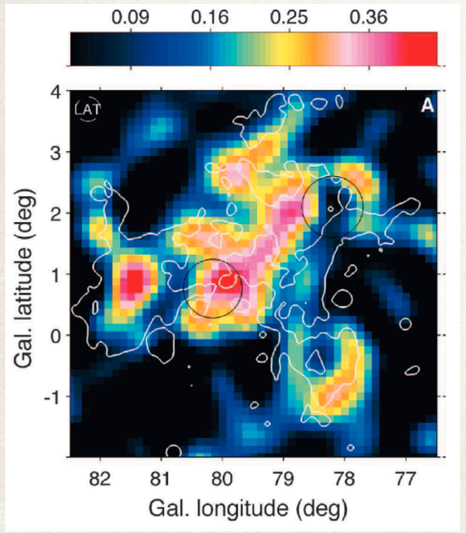

HAWC

Abeysakara et al. (2021) Nat. Astron.

Power law spectral energy index
s~2.3 below ~TeV

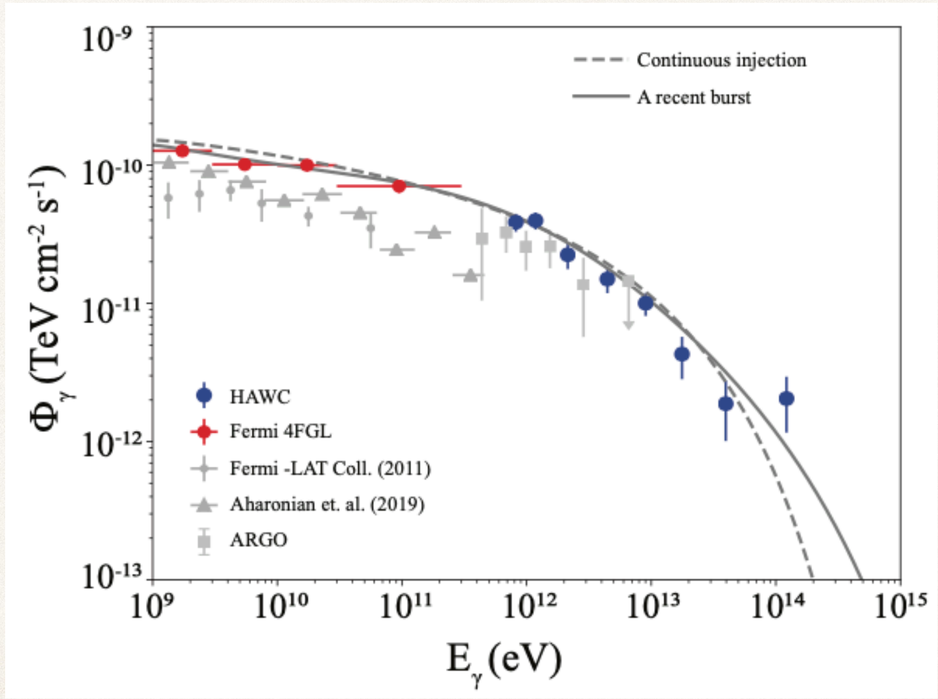

Spatial profile:

- centrally peaked at low energies (>100 GeV)
- flat at high energies (> 10 TeV)

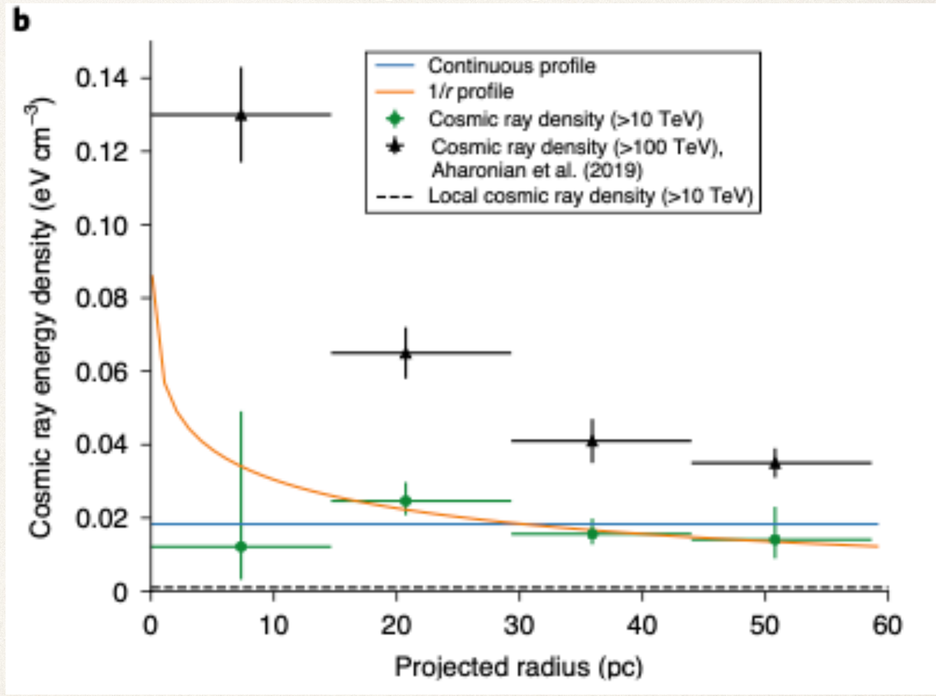

Fermi-LAT

Ackermann et al. (2011) Science 334

OBSERVATIONS: Westerlund 1

Mohrmann et al. (2021) ICRC proceeding, arXiv2108.03003

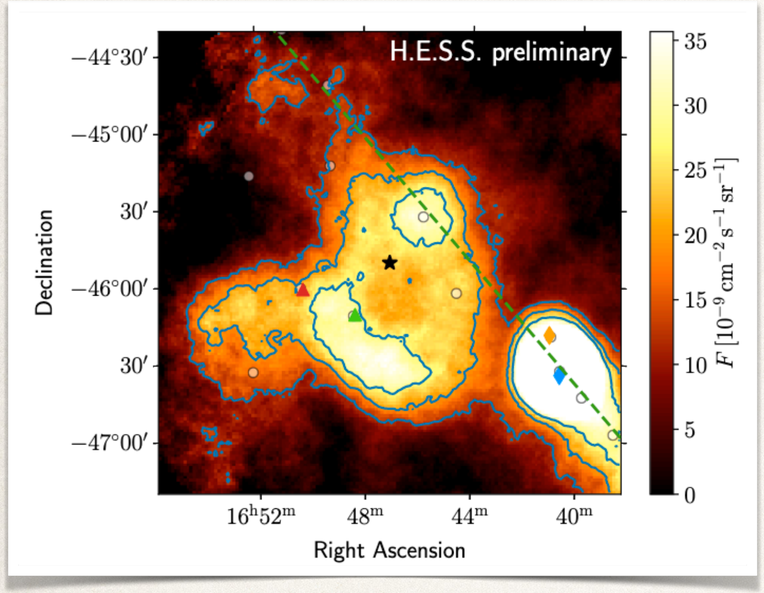

HESS preliminary analysis

- Complex morphology
- No signifiant variation with energy
- Energy spectral index ~2.4

Spatial profile

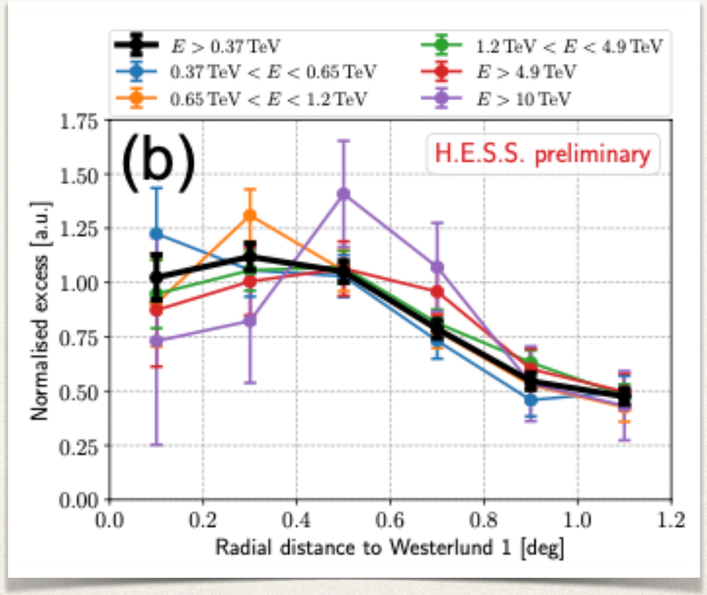

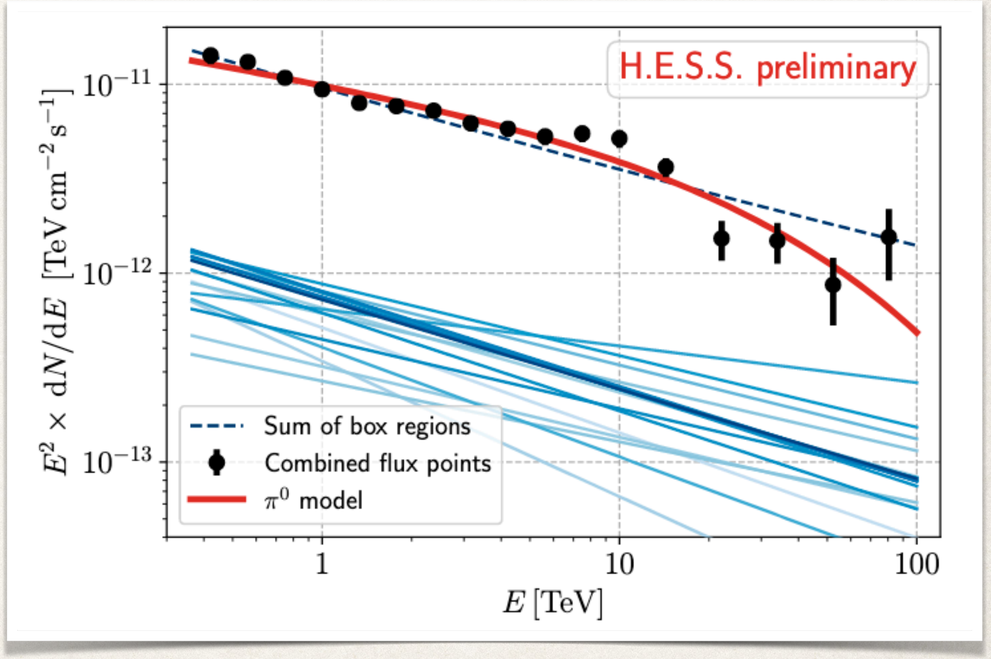

OBSERVATIONS: Westerlund 2

HESS significance map

HESS collaboration, A&A 525 A46 (2011)

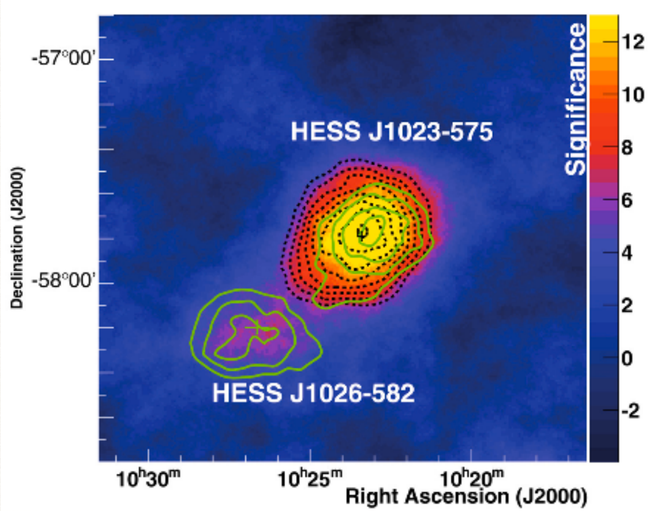

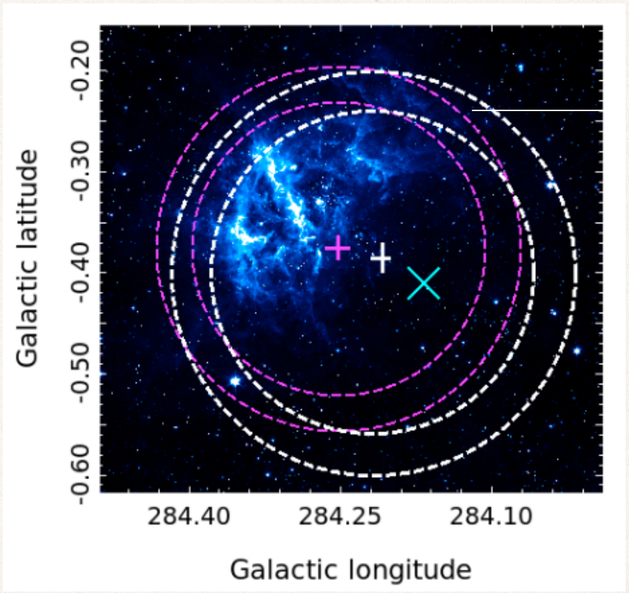

Spitzer/IRAC mosaic
J1023-575(HESS; white)
J1023.3-5747 (Fermi-LAT; magenta)
cyan cross: pusar

- Compatible size in GeV and TeV range
- Spectral slope ~2 @ $E <$ TeV; 2.6 @ $E >$ TeV
- PWN contribution disfavoured
- Most promising accelerator in the FoV is Westerlund 2
- Total gamma-ray luminosity ~0.2% of mechanical wind energy

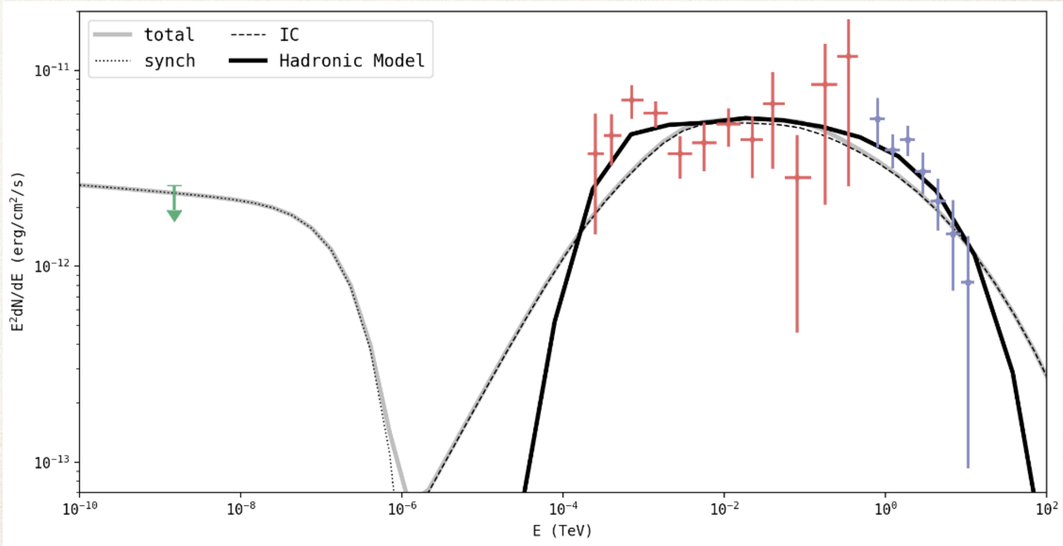

Mestre et al. (2021) MNRAS, 502, 2

Possible acceleration mechanisms

Young Stellar clusters (no SNRs)

- Wind-wind collision [Reimer, Pohl, Reimer (2006); Bykov, Gladilin & Osipov (2013); Vieu, Gabici & Tatischeff (2020)]
- Termination shock of single stars
- **Collective wind termination shock** [GM et al. 2021]

Superbubbles (Winds+SNRs)

- DSA in enhanced turbulence [Parizot et al. 2004]
- Multiple primary shocks [Klepach et al. 2000]
- Multiple primary and secondary shocks [Bykov & Toptygin 1982, Bykov & Fleishman 1992]
- Acceleration by turbulence [Bykov & Toptygin 1993]
- Turbulence + multiple shocks [Parizot et al. 2004; Ferrand & Markowith 2010; Vieu, Gabici & Tatischeff ICRC 2021]

The wind-bubble system

The stellar wind blow a hot bubble in the ISM [Weaver et al., 1977, ApJ 218]

- The hot bubble spend the majority of its life (~few Myr) the in adiabatic phase
- The shocked ISM collapse to a thin shell ($t_{\rm cool} \sim 10^4\, yr$)
- The termination shock is almost stationary

Bubble radius:

$$R_b \simeq 55\ {\rm pc} \left(\frac{\dot{M}}{10^{-4} M_\odot/yr}\right)^{1/5} \left(\frac{v_w}{1000\,{\rm km/s}}\right)^{2/5} \left(\frac{\rho_0/m_p}{{\rm cm}^{-3}}\right)^{-1/5} \left(\frac{t_{\rm age}}{\rm Myr}\right)^{3/5}$$

Radius of termination shock:

$$R_s \simeq 20\ {\rm pc} \left(\frac{\dot{M}}{10^{-4} M_\odot/yr}\right)^{3/10} \left(\frac{v_w}{1000\,{\rm km/s}}\right)^{1/10} \left(\frac{\rho_0/m_p}{{\rm cm}^{-3}}\right)^{-3/10} \left(\frac{t_{\rm age}}{\rm Myr}\right)^{2/5}$$

$u_{ts} \simeq v_w \sim 2000 - 3000\,{\rm km/s}$

$u_{fs} = \dfrac{dR_b}{dt} \simeq 10 - 30\,{\rm km/s}$

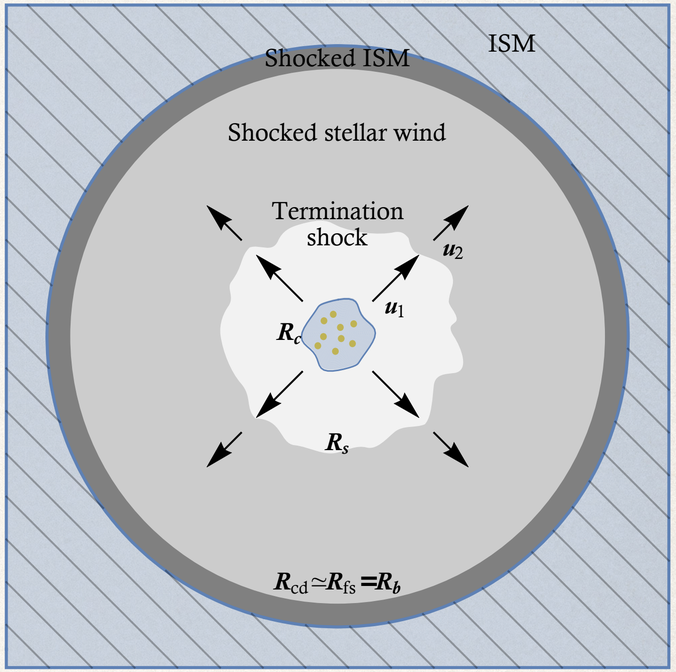

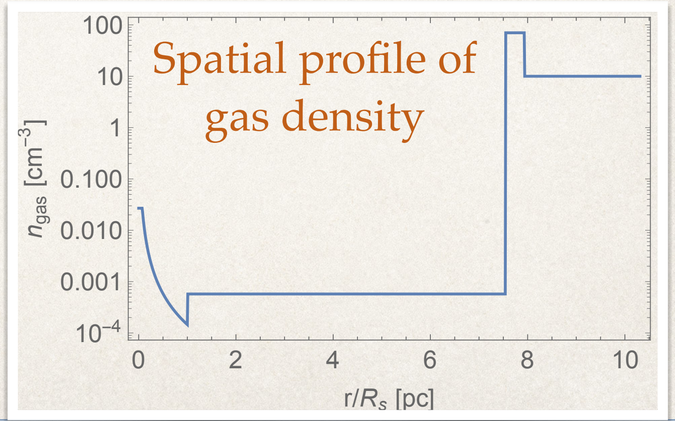

Cluster compactness

In general a large scale termination shock is generated if the cluster is compact enough, such that $R_{\rm cluster} \ll R_{\rm ts}$

$$R_{\rm ts} = \sqrt{\frac{L_w}{2\pi v_w P_{\rm bubble}}}$$

From the model by Chevalier & Clegg (1985)

$$R_{\rm ts} \simeq 20\ {\rm pc} \left(\frac{\dot{M}}{10^{-4} M_\odot/yr}\right)^{\frac{3}{10}} \left(\frac{v_w}{1000\,{\rm km/s}}\right)^{\frac{1}{10}} \left(\frac{\rho_0/m_p}{{\rm cm}^{-3}}\right)^{-\frac{3}{10}} \left(\frac{t_{\rm age}}{\rm Myr}\right)^{\frac{2}{5}}$$

Powerful clusters should easily produce a large scale termination shock

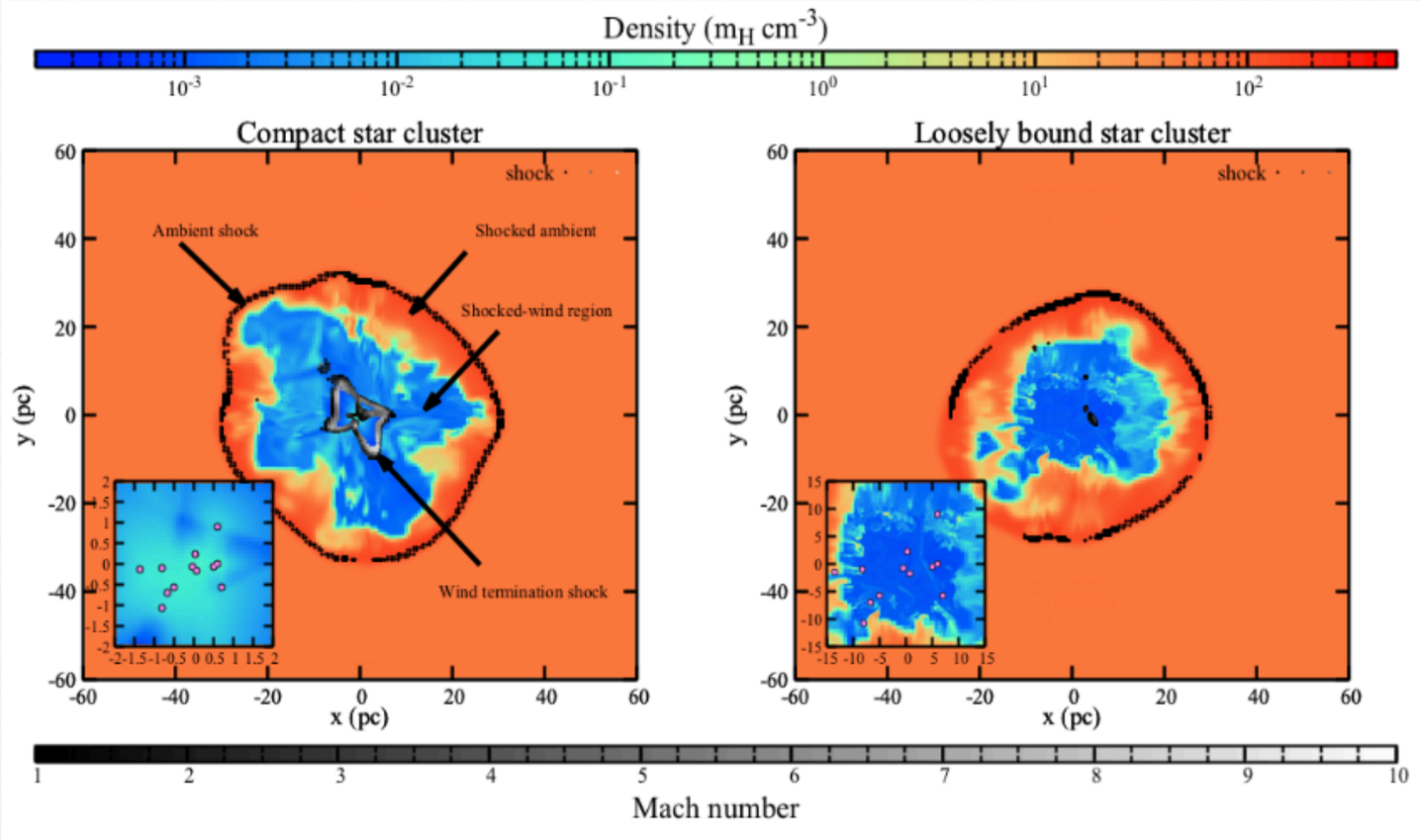

[Gupta, Nath, Sharma & Eichler, MNRAS 2020]

Particle acceleration at the termination shock

Time-stationary transport equation in spherical geometry:

$$\frac{\partial}{\partial r}\left[r^2 D(r,p)\frac{\partial f}{\partial r}\right] - r^2 u(r)\frac{\partial f}{\partial r} + \frac{d\left[r^2 u\right]}{dr}\frac{p}{3}\frac{\partial f}{\partial p} + r^2 Q(r,p) = 0$$

- Arbitrary diffusion coefficient $D(\mathrm{r},p)$
- Injection only at the termination shock $\quad Q(r,p) \propto \delta(p - p_{\mathrm{inj}})\,\delta(r - R_s)$
- Wind velocity profile: $\quad u(r) = \begin{cases} u_1 = v_w & \text{for } r < R_s\,, \\ \dfrac{u_1}{\sigma}\left(\dfrac{R_s}{r}\right)^2 & \text{for } R_s < r < R_b\,, \\ 0 & \text{for } r > R_b\,; \end{cases}$

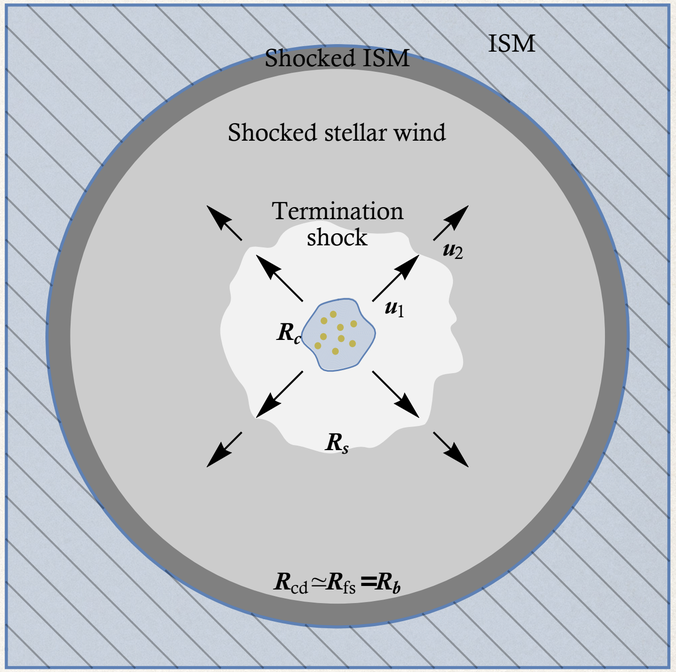

With respect to SNRs the geometry is “reversed”

Solution of the transport equation

Time-stationary transport equation in spherical geometry:

$$\frac{\partial}{\partial r}\left[r^2 D(r,p)\frac{\partial f}{\partial r}\right] - r^2 u(r)\frac{\partial f}{\partial r} + \frac{d\left[r^2 u\right]}{dr}\frac{p}{3}\frac{\partial f}{\partial p} + r^2 Q(r,p) = 0$$

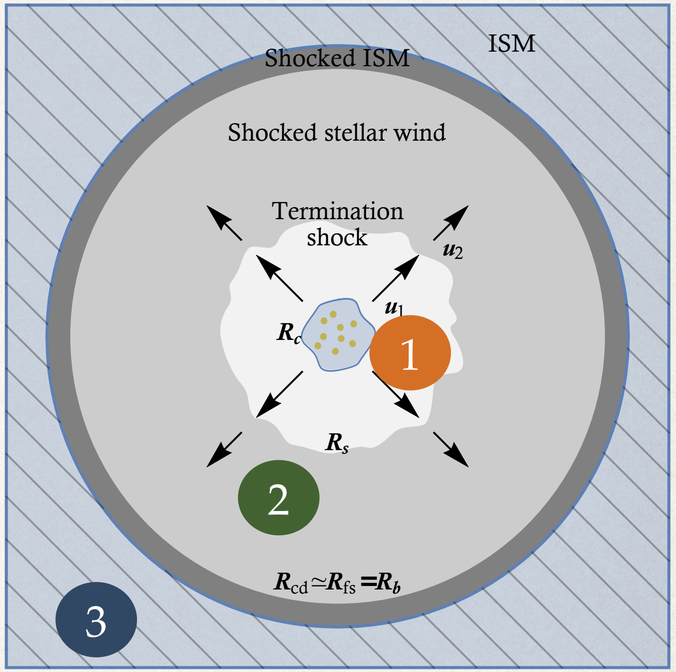

Boundary conditions:

1. No net flux at the cluster center: $r^2[D\partial_r f - uf]_{r=R_c} = 0$

2. Matching the Galactic distribution: $f(r \to \infty, p) = f_{\rm gal}(p)$

- The equation is solved in regions 1, 2 and 3 and than matched at $R_{\rm s}$ and $R_{\rm b}$ using the flux conservation

- For generic expression of $D(r,p)$ and $u(r)$ the solution is not analytical, but can be expressed in an implicit form that can be solved by iterations.

Diffusion coefficient

Time-stationary transport equation in spherical geometry:

$$\frac{\partial}{\partial r}\left[r^2 D(r,p)\frac{\partial f}{\partial r}\right] - r^2 u(r)\frac{\partial f}{\partial r} + \frac{d\left[r^2 u\right]}{dr}\frac{p}{3}\frac{\partial f}{\partial p} + r^2 Q(r,p) = 0$$

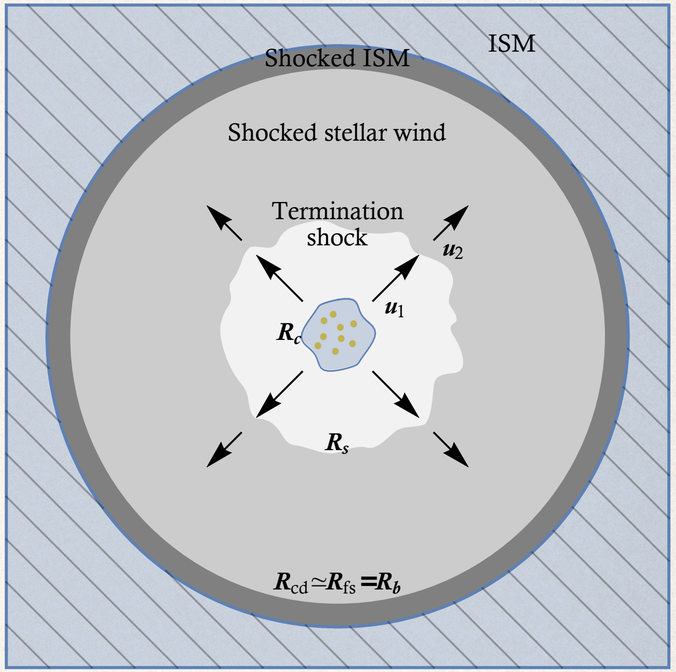

Wind-wind collision and non-stationarity can produce high level of HD turbulence

Assuming that a fraction η_B of kinetic wind energy is converted into magnetic energy

$$\frac{\delta B}{4\pi} 4\pi r^2 v_w = \frac{1}{2}\eta_B \dot{M} v_w^2 \Rightarrow \delta B(R_s) \gtrsim \mu G$$

The type of turbulent cascade can result into different diffusion coefficients

$$\begin{cases} D_{\rm Kol}(E) = \frac{v}{3} r_L (\delta B)^{1/3} L_c^{2/3} \\ D_{\rm Kra}(E) = \frac{v}{3} r_L (\delta B)^{1/2} L_c^{1/2} \\ D_{\rm Bohm}(E) = \frac{v}{3} r_L (\delta B) \end{cases}$$

L_c is the injection scale of turbulence, assumed of the order of the cluster size (~pc)

Bohm diffusion can be realised if there are multiple injection scales

Solution: particle distribution at the shock

$$f_s(p) = s \frac{\eta_{\rm inj} n_1}{4\pi p_{\rm inj}^3} \left(\frac{p}{p_{\rm inj}} \right)^{-s} e^{-\Gamma_1(p)} \; e^{-\Gamma_2(p)}$$

Solution: particle distribution at the shock

Standard power-law for plane shocks

$$s = \frac{3u_1}{u_1 - u_2}$$

$$f_s(p) = s\frac{\eta_{\rm inj}\, n_1}{4\pi\, p_{\rm inj}^3}\left(\frac{p}{p_{\rm inj}}\right)^{-s} e^{-\Gamma_1(p)} \quad e^{-\Gamma_2(p)}$$

Solution: particle distribution at the shock

Standard power-law for plane shocks

$$s = \frac{3u_1}{u_1 - u_2}$$

$$f_s(p) = s\frac{\eta_{\rm inj}\, n_1}{4\pi\, p_{\rm inj}^3}\left(\frac{p}{p_{\rm inj}}\right)^{-s} e^{-\Gamma_1(p)}\; e^{-\Gamma_2(p)}$$

Where:

$$\Gamma_1(p) = s\int_{p_{\rm inj}}^{p} \frac{\Lambda_1(1,p')}{f_s(p')}dp' \quad \Rightarrow \quad \Gamma_1(p) \gg 1 \Rightarrow p \gg p_{\rm max\,1} : \frac{D_1(p_{\rm max\,1})}{u_1} = R_s$$

$p_{\rm max}$ due to the upstream: the effective plasma speed decreased reducing the energy gain

$$\Lambda_1(\xi,p) = -\frac{2}{3}\int_0^{\xi} f_1(\xi',p)\frac{d\ln(p^3 f_1)}{d\ln p}\xi' d\xi' \quad \Rightarrow$$

Non-linear term:
f_s depends on f_1 (upstream)

Solution: particle distribution at the shock

Standard power-law for plane shocks

$$s = \frac{3u_1}{u_1 - u_2}$$

$$f_s(p) = s\frac{\eta_{\rm inj} n_1}{4\pi p_{\rm inj}^3}\left(\frac{p}{p_{\rm inj}}\right)^{-s} e^{-\Gamma_1(p)} e^{-\Gamma_2(p)}$$

Where:

$$\Gamma_1(p) = s\int_{p_{\rm inj}}^{p} \frac{\Lambda_1(1,p')}{f_s(p')}dp' \quad \Rightarrow \quad \Gamma_1(p) \gg 1 \Rightarrow p \gg p_{\rm max\,1} : \frac{D_1(p_{\rm max\,1})}{u_1} = R_s$$

$p_{\rm max}$ due to the upstream: the effective plasma speed decreased reducing the energy gain

$$\Lambda_1(\xi,p) = -\frac{2}{3}\int_0^{\xi} f_1(\xi',p)\frac{d\ln(p^3 f_1)}{d\ln p}\xi' d\xi' \quad \Rightarrow$$

Non-linear term:
f_s depends on f_1 (upstream)

$$\Gamma_2(p) = s\frac{u_2}{u_1}\int_{p_{\rm inj}}^{p} \frac{dp'/p'}{e^{\alpha_2(p',R_b)} - 1} \quad \Rightarrow \quad \Gamma_2(p) \gg 1 \Rightarrow p \gg p_{\rm max\,2} : \int_{R_s}^{R_b} \frac{u(r)dr}{D(p_{\rm max})} = 1$$

$p_{\rm max}$ due to the escape from the downstream

Impact of diffusion coefficient

For fixed values of all parameters, the diffusion coefficient has a strong impact on the cutoff shape and effective maximum energy

Typical values for massive stellar clusters

$$\begin{cases} \dot{M} = 10^{-4}\, M_\odot\, \mathrm{yr}^{-1} \\ v_w = 3000\ \mathrm{km/s} \\ L_{\mathrm{CR}} = 0.1\, L_w \\ \eta_B = 0.1 \end{cases}$$

PeV energies can be reached in very powerful stellar clusters if the diffusion is close to *Bohm*

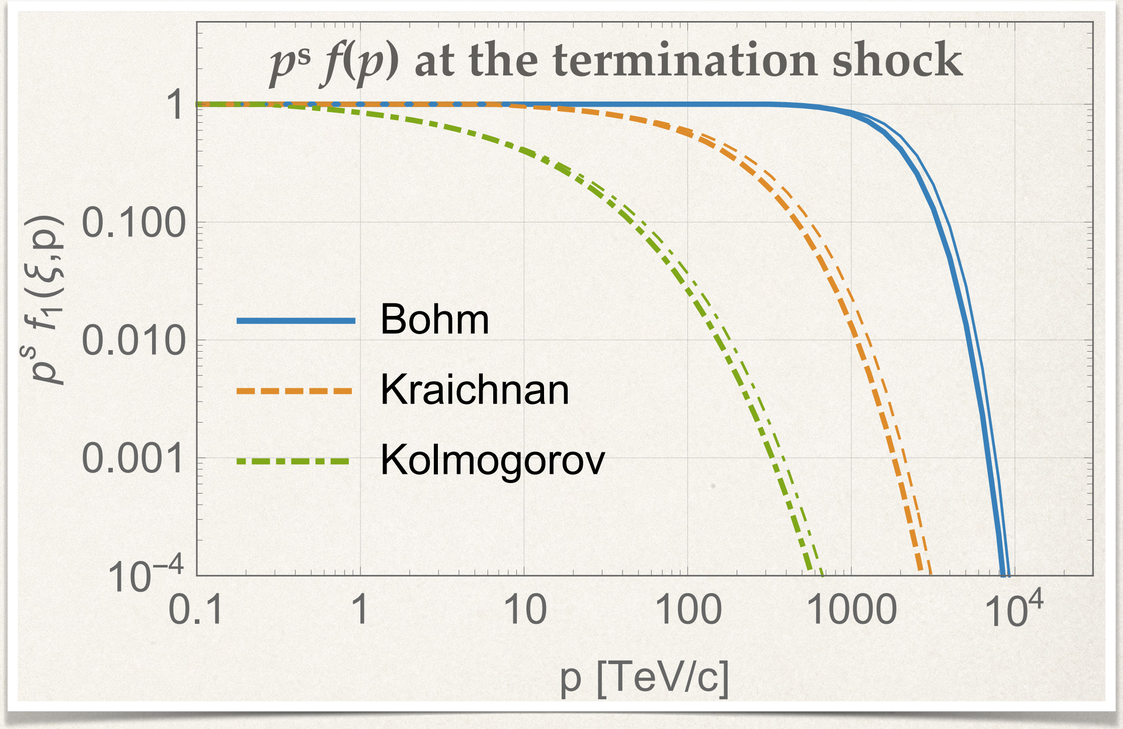

Determining the diffusion properties inside the bubble is fundamental

Solution: spatial profile of CR distribution

Region 1 (cold wind):

$$f_1(\xi,p) = f_s(p)\,\exp\left\{-\int_\xi^1 \alpha_1\left[1+\frac{\Lambda_1(\xi',p)}{\xi'^2 f_1(\xi',p)}\right]d\xi'\right\}$$

Region 2 (shocked wind):

$$f_2(\xi,p) = f_s(p)\,e^{\alpha_2}\,\frac{1+\beta\left[e^{\alpha_2(1)-\alpha_2(\xi)}-1\right]}{1+\beta\left[e^{\alpha_2(1)}-1\right]} + f_{\rm gal}(p)\,\frac{\beta\left[e^{\alpha_2(\xi)}-1\right]}{1+\beta\left[e^{\alpha_2(1)}-1\right]}$$

Region 3 (unperturbed ISM):

$$f_3(\xi,p) = f_2\left(R_b/R_s,p\right)\frac{1}{\xi} + f_{\rm gal}(p)\left(1-\frac{1}{\xi}\right)$$

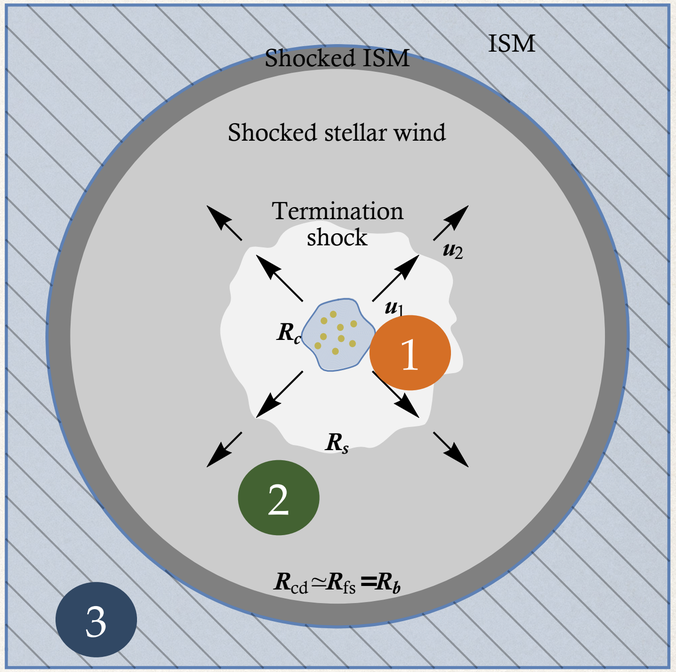

where: $\xi = \dfrac{r}{R_s}$; $\alpha_1(\xi,p) = \dfrac{u_1 R_s}{D_1(\xi,p)}$; $\alpha_2(\xi,p) = \dfrac{u_2 R_s}{D_2(p)}\left(1-\dfrac{1}{\xi}\right)$; $\beta(p) = \dfrac{D_{\rm gal}(p) R_s}{u_2 R_b^2}$;

Solution: spatial profile of CR distribution

- For $r < R_s$ the distribution is suppressed except when $E \gtrsim E_{\rm max}$
- Distribution inside the bubble is flat for $E \ll E_{\rm max}$
  - $\neq 1/r$ inferred from FermiLAT data by Aharonian et al., 2019, Nat. Astr.3, 561
- For $E \lesssim 100 GeV$ the distribution outside the bubble is larger than the one inside it
  - possible signature in the gamma-ray emission (to be investigated)

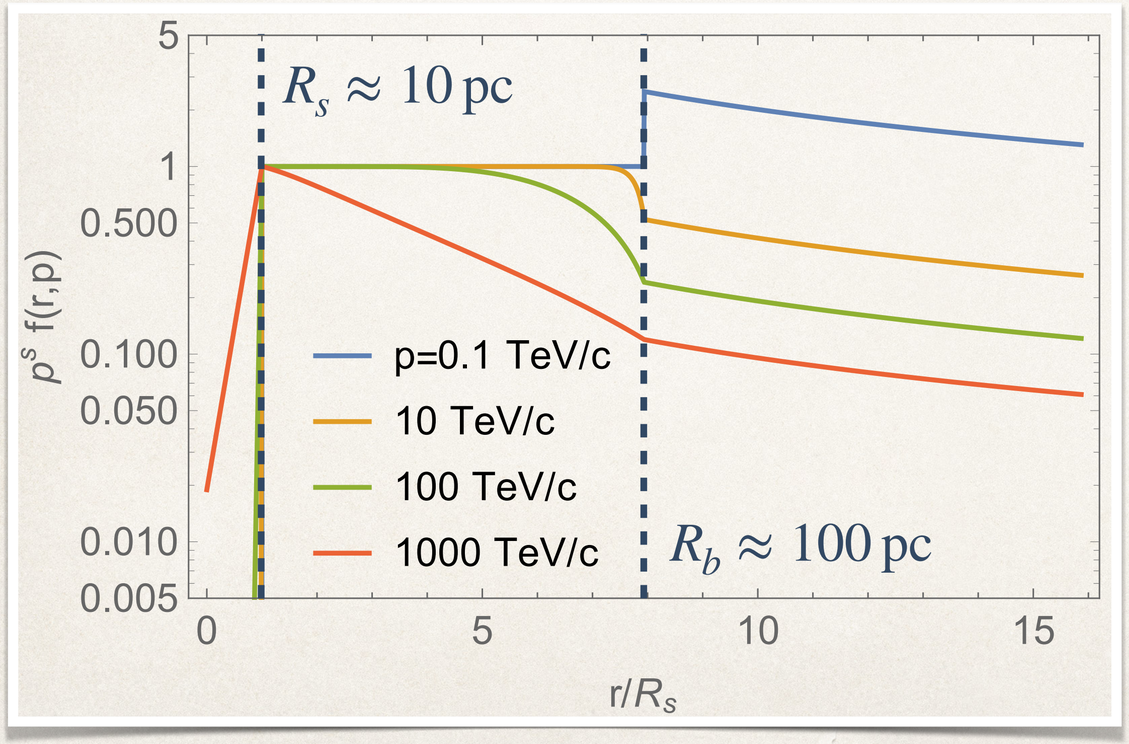

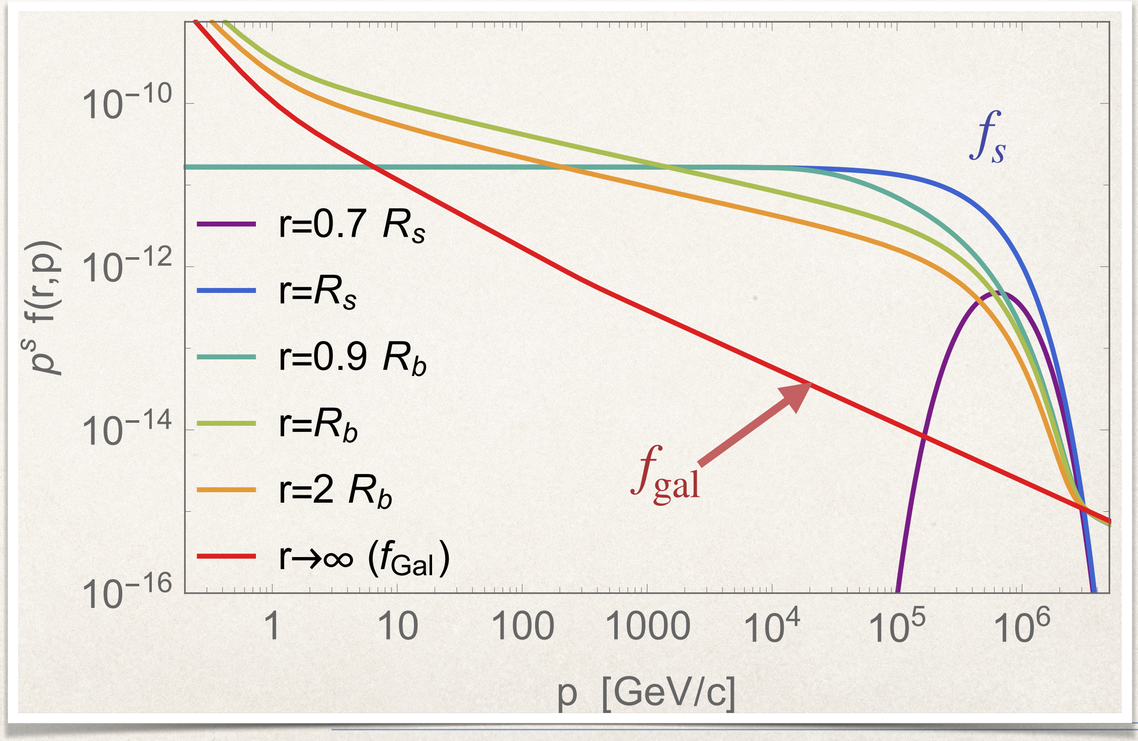

Source of turbulence: Colliding winds in binaries

[Bosh-Ramon, Brrkov & Perucho, A&A 2015]

- Colliding wind binaries show evidence of particle acceleration
- Turbulence injection on scale comparable to stellar distance due to stellar orbital motion

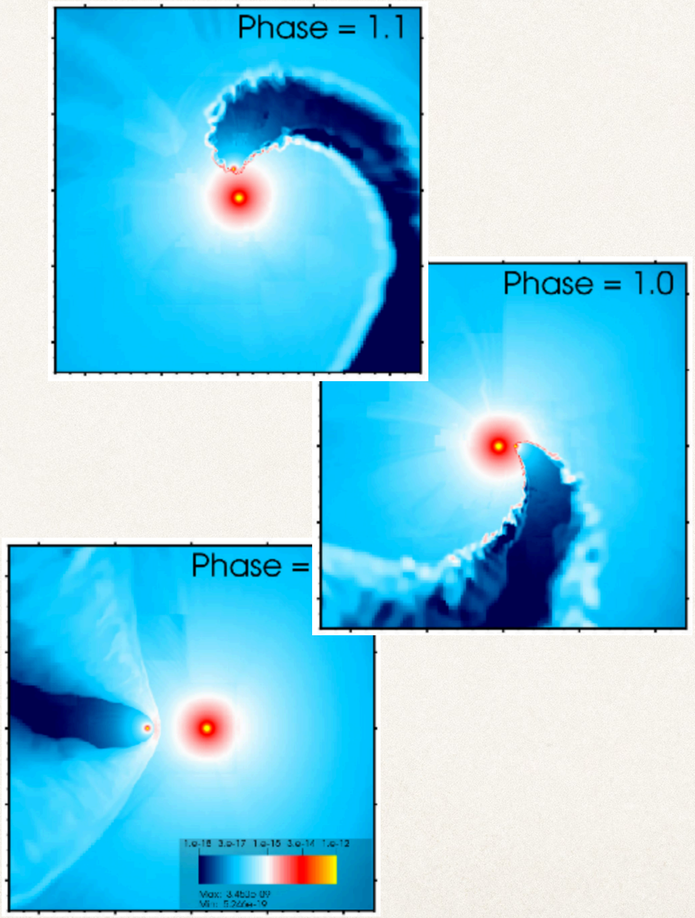

VLBA 3.6 cm observation of WR 140

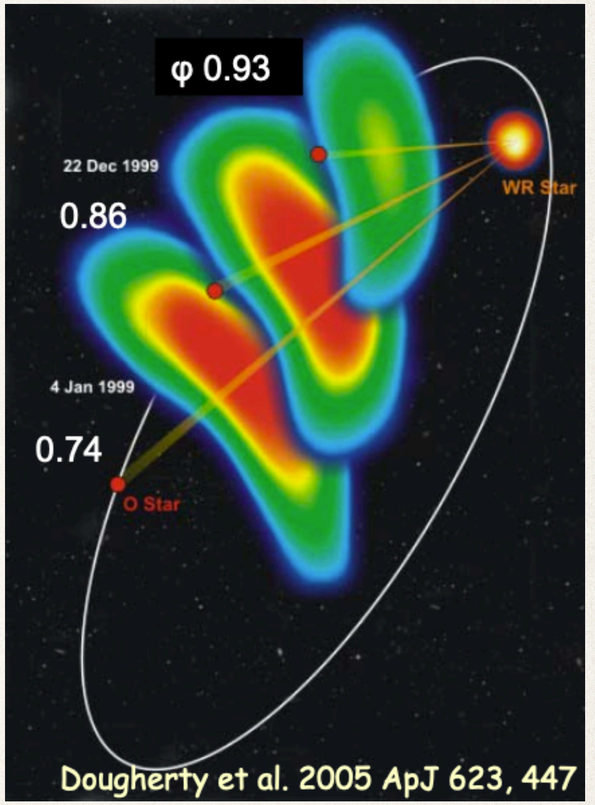

3D simulation of WR+O colliding wind binaries [Parkin & Grosset, 2011

Possible role of self-generated magnetic field

Similarly to what is thought to happen for SNR shocks, streaming CRs could amplify the turbulent magnetic field ahead of the shock through resonant or non-resonant modes

Resonant modes

$$\left(\frac{\delta B_{\rm res}}{B_1}\right)^2 \simeq \frac{\pi}{2}\frac{\xi_{\rm CR}}{p_{\rm max}/m_p c}\frac{v_w}{v_A} = \frac{\pi}{2}\frac{\xi_{\rm CR}}{p_{\rm max}/m_p c}\frac{1}{\sqrt{2\eta_B}} \quad \Rightarrow \quad \delta B_{\rm res} > B_1 \quad \text{only if} \quad \eta_B \lesssim 10^{-4} \quad \Rightarrow \quad \delta B_{\rm res} \ll \mu G$$

Non-resonant modes

Allowed to grow only if energy density in CR current > energy density of pre-existing magnetic field

$$\Rightarrow \quad \eta_B \lesssim \frac{6\,\xi_{\rm CR}}{\log(p_{\rm max}/m_p c)}\frac{v_w}{c} \sim 10^{-4} \quad \Rightarrow \quad \delta B_{\rm non-res} \ll \mu G$$

CR self-amplification is not efficient

Conclusions

Context:

- Several massive stellar clusters have been associated to gamma-ray sources, suggesting that they could contribute to the bulk of Galactic component of cosmic rays.
- **Where those particles are accelerated?**

Method:

- We investigated the spectrum of protons accelerated at the termination shock of stellar winds, developing a technique to solve the transport equation in spherical symmetry able to account for *space-dependent* wind velocity and *space-* and *energy-dependent* particle diffusion.

Results:

- The maximum energy can reach the PeV for very massive stellar cluster under the assumption that few percent of the wind kinetic energy is converted into magnetic turbulence and that diffusion is close to *Bohm*.
- The spatial profile of the accelerated particles is almost flat in the bubble

Acceleration in super-bubbles

[e.g Higdon & Lingenfelter 2003, Parizot et al. 2004]

- Simultaneous presence of stellar winds and SNe
- Acceleration by multiple repeated shocks
- Fermi II order acceleration by turbulence

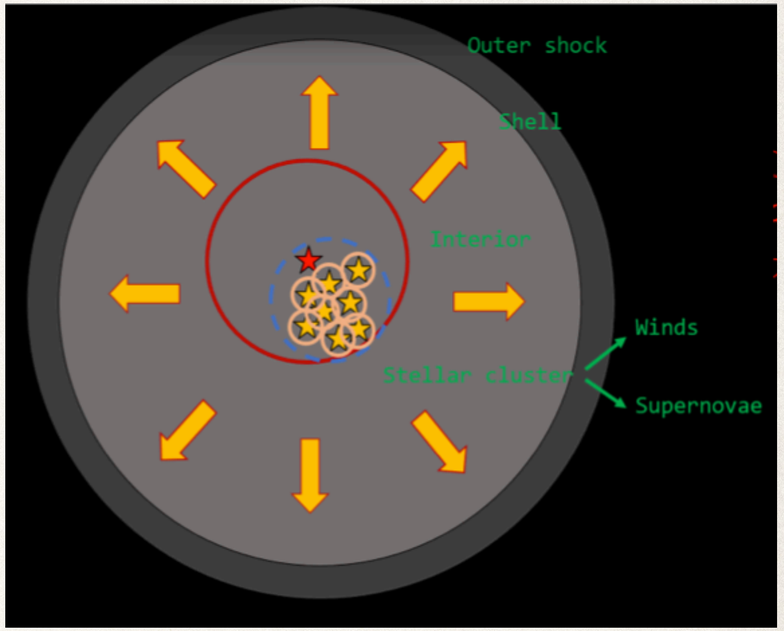

Particle acceleration due to multiple shocks and turbulence

[Bykov & Fleishman 1992]

A general feature of acceleration models including turbulence and multiple shocks is the hard spectrum (≤ 3) below some characteristic energy

For example in the model by Bykov & Toptigyn (1992) the particle spectrum is

$$f_p(p) \propto \begin{cases} \left(\frac{p}{p_i}\right)^{-3}, & \text{for } p_i < p < p^*; \\ \left(\frac{p^*}{p_i}\right)^{\alpha-3} \left(\frac{p}{p_i}\right)^{-\alpha} & \text{for } p^* < p < p_1; \end{cases}$$

Collective reacceleration occurs below $p^* \simeq p_i\, e^{t/t_{\rm ch}}$ where $t_{\rm ch} = l_c/u_T$

Maximum value of p^* determined from energy equipartition

$$W_{\rm cr} < W_{\rm th} \Rightarrow p_* < m_p c \eta^{-1} (u/c)^2 \approx 1\,{\rm GeV}/c \frac{10^{-5}}{\eta} \left(\frac{u}{1000\,{\rm km/s}}\right)^2$$

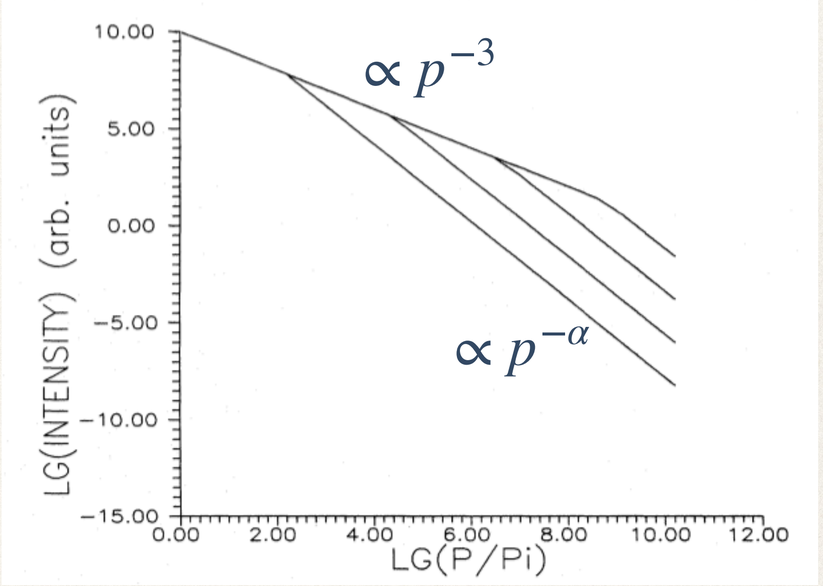

From Bykov & Fleishman 1992

Particle acceleration due to multiple shocks and turbulence

[Vieu, Gabici & Tatischeff, ICRC 2021]

- Time dependent model accounting for winds, SNRs and turbulence.
- The intermittency of SN explosion produces a large variation of CR content in SBs
- Maximum energy dominated by SNR; turbulence affects only $E \lesssim 1\,\mathrm{GeV}$
- Particle escape from the super bubble results in steep spectra $\sim E^{-2.2}$

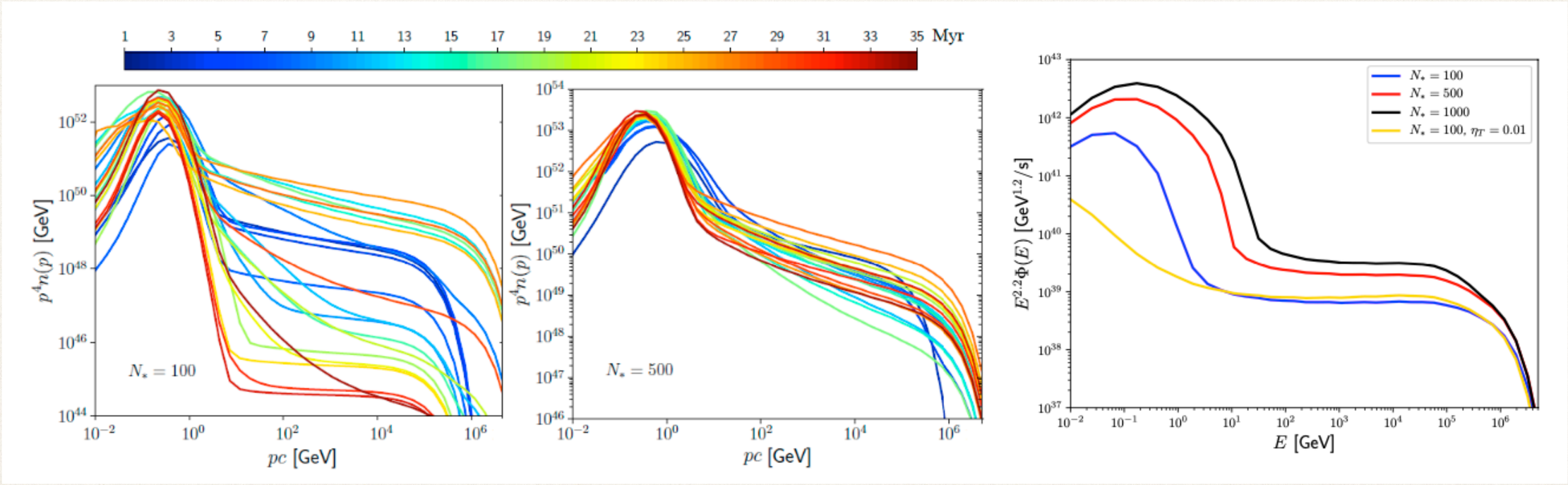

CR spectra at various times for a typical cluster of 100 massive stars (left), and 500 massive stars (center). The right panel displays the average escaping fluxes.

Shell fragmentation

[Lancaster et al., ApJ 914, 89 (2021)]
[Lancaster et al., ApJ 914, 90 (2021)]

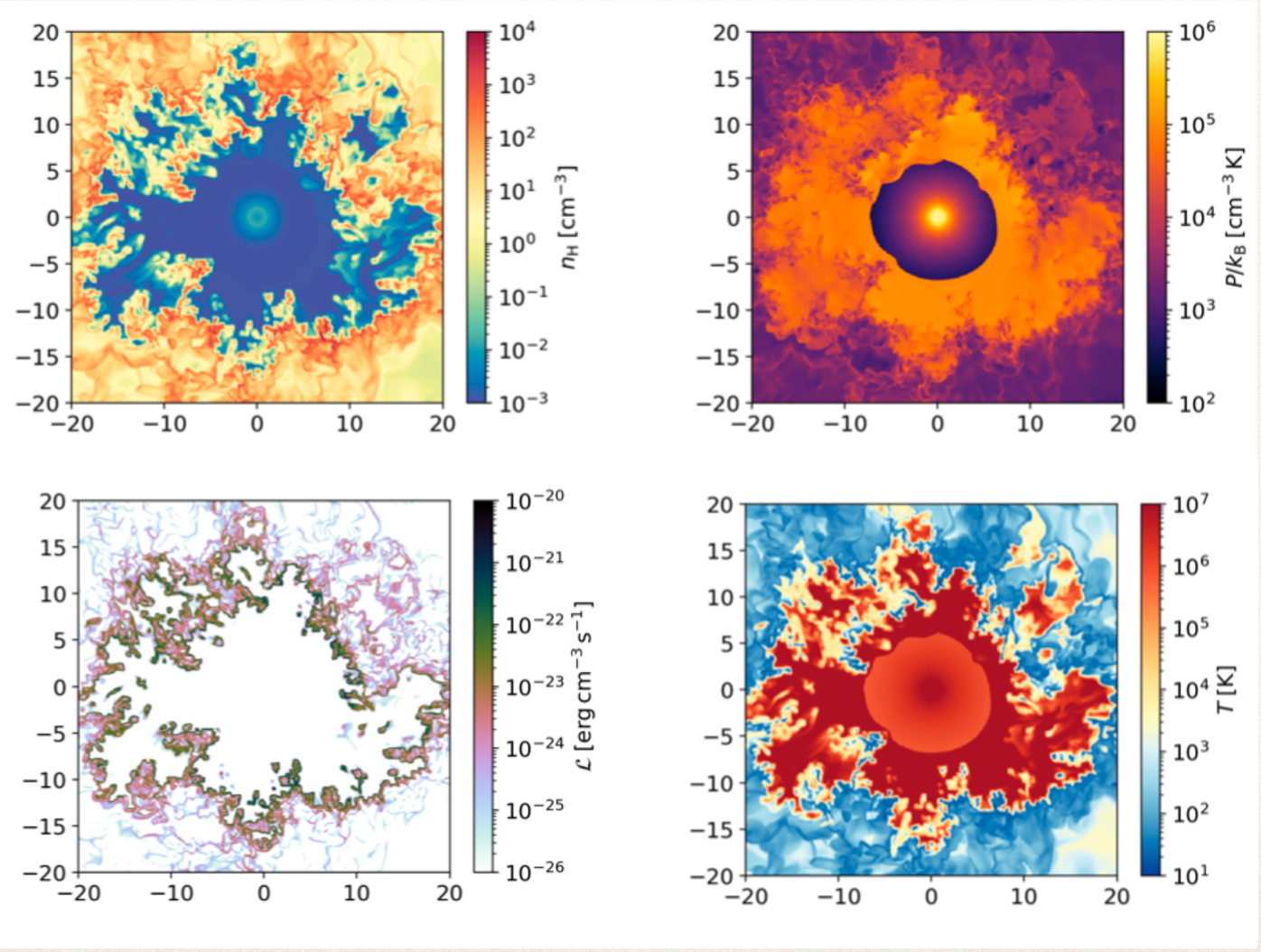

Rayley-Taylor instability between dense ISM and low density bubble produces a fragmentation of the shocked ISM shell.

- Fragmentation enhances the cooling rate
  - The bubble effective size is reduced
- Dense clouds are located inside the bubble
  - gamma-ray emission possible also from the bubble interior
- What is the effect on CR diffusion?

3D Hydrodynamic simulations

$M_{\rm cloud} = 10^5 M_\odot$
$\mathscr{L}_w/M_* = 10^{34} {\rm erg\,s^{-1}} M_\odot^{-1}$
$t_{\rm age} = 2.23 {\rm Myr}$
$R_{\rm cloud} = 20\,{\rm pc}$

Open questions

- **Which is the main acceleration mechanism?**
  - wind-wind collisions
  - turbulent acceleration
  - wind termination shocks
- **Which is the maximum possible energy of accelerated particles?**
  - strong dependence on magnetic field strength and turbulence power
- **Study of turbulence**
  - which observations?
  - need of specific numerical simulations
  - role of realistic environments (fragmentation; cooling)
- **Chemical composition:** Can CR from stellar winds help to account for anomalous CR chemical composition?
- **Can stellar winds significantly contribute to Galactic CRs?** Which is the total contribution integrated over the stellar clusters population?